3. G. H. Recanzone, M. M. Merzenich, W. M. Jenkins, K. A. Grajski, H. R. Dinse, *J. Neurophysiol.* **67**, 1031 (1992).
4. T. A. Woolsey and H. Van der Loos, *Brain Res.* **17**, 205 (1971); C. Welker, *ibid.* **26**, 259 (1971); M. Armstrong-James, K. Fox, A. Das-Gupta, *J. Neurophysiol.* **68**, 1345 (1992).
5. M. E. Diamond, M. Armstrong-James, F. F. Ebner, *Proc. Natl. Acad. Sci. U.S.A.* **90**, 2602 (1993); M. Armstrong-James, M. E. Diamond, F. F. Ebner, *J. Neurosci.*, in press.
6. In experimental subjects, whiskers on the right side (except the paired whiskers) were clipped to a length of 2 to 3 mm; whiskers on the left side were not cut. The data from experimental subjects with whiskers D2 and D1 paired (four cases) and whiskers D2 and D3 paired (four cases) were combined because no significant differences were found when evaluated separately; also, see (*5*).
7. Body temperature was maintained at 36° to 37°C. Anesthesia was held at a consistent depth by maintaining the burst rate of layer V neurons at 2 to 4 Hz. When anesthetic depth decreased, a supplement of urethane was given (10% of the original dose).
8. The horizontal location of a recording site is critical because in normal rats the receptive-field symmetry of barrel D2 neurons is correlated with their horizontal location (*5*). After a microelectrode penetration was completed, an electrolytic lesion (positive direct current of 0.2 μA for 5 s) was made at a depth of 500 to 700 μm for visualization by cytochrome oxidase staining. At the end of the experiment, rats received pentobarbitol (50 mg/kg, intraperitoneally) and were perfused. The neocortex was separated from the white matter and flattened between glass slides. The slab was frozen and 50-μm tangential sections were processed for cytochrome oxidase activity. The points at which penetrations passed through layer IV of column D2 were projected onto the tangential barrel map.
9. Individual whiskers were deflected by a wire tip glued to a piezoelectric ceramic wafer positioned just below the whisker, 2 mm from the skin. The stimulus, delivered at 1 Hz, was a ~300-μm up-down movement of the tip with a total duration of 3 ms. Action potentials were recorded by carbon-fiber microelectrodes and isolated by a window discriminator. With the use of peristimulus time and latency histograms with 1-ms bins, the response to whisker deflection was measured on-line (CED 1401) and stored. To calculate the evoked sensory response, the number of spikes occurring in the first 100 ms after the stimulus was counted and adjusted by subtraction of the number of spikes occurring in the 50 ms preceding the whisker deflections (an estimate of spontaneous activity), multiplied by two.
10. In pilot experiments, small electrolytic lesions were made at measured depths and later examined in coronal, cytochrome-oxidase–stained sections. The granular layer (layer IV) could be reliably identified at the in vivo depth of 400 to 800 μm. Thus, 62 neurons (27 in normal cases, 35 in experimental cases) were classified as supragranular, 110 neurons (65 in normal cases, 45 in experimental cases) as granular, and 53 neurons (27 in normal cases, 26 in experimental cases) as infragranular. Layers II to III were grouped together, as were layers V to VI.
11. The response in the supragranular layers to D-paired increased ($t = 3.581$, $P < 0.005$), whereas the response to D-cut did not change ($t = 0.475$, $P = 0.636$). In the infragranular layers, the response to D-paired increased ($t = 2.032$, $P < 0.05$), whereas the response to D-cut did not change ($t = 0.100$, $P = 0.920$). In layer IV, neither the response to D-paired nor the response to D-cut changed ($t = -0.488$, $P = 0.626$ and $t = -0.192$, $P = 0.848$, respectively).
12. Local connections in rodent somatosensory cortex are described in J. K. Chapin, M. Sadeq, J. L. U. Guise, *J. Comp. Neurol.* **263**, 326 (1987); K. L. Bernardo, J. S. McCasland, T. A. Woolsey, R. N. Strominger, *ibid.* **291**, 231 (1990); M. A. L. Nicolelis, J. K. Chapin, C. S. Lin, *Somatosens. Mot. Res.* **8**, 193 (1991); U. Kim and F. F. Ebner, *Soc. Neurosci. Abstr.* **19**, 107 (1993).
13. N. D. Akhtar and P. W. Land, *J. Comp. Neurol.* **307**, 200 (1991).
14. M. A. L. Nicolelis, R. C. S. Lin, D. J. Woodward, J. K. Chapin, *Nature* **361**, 533 (1993).
15. M. B. Calford and R. Tweedale, *Proc. R. Soc. London* **243**, 269 (1991).
16. M. Armstrong-James, E. Welker, C. A. Callahan, *J. Neurosci.* **13**, 2149 (1993). Spikes evoked in the subsequent 90-ms interval are produced mainly through intracortical circuits.
17. D. O. Hebb [*The Organization of Behavior: A Neuropsychological Theory* (Wiley, New York, 1949)] proposed that the connection from cell A to cell B will be potentiated if cell A "repeatedly or persistently takes part in firing" cell B.
18. P. Zarzecki *et al.*, *J. Neurophysiol.* **69**, 1422 (1993). Additional evidence for Hebbian-type intracortical potentiation is found in rat somatosensory cortex [J. Delacour, O. Houcine, B. Talbi, *Neuroscience* **23**, 63 (1987)], monkey auditory cortex [E. Ahissar *et al.*, *Science* **257**, 1412 (1992)], cat and guinea pig visual cortex in vitro [Y. Frégnac, J. P. Burke, D. Smith, M. J. Friedlander, *J. Neurophysiol.* **71**, 1403 (1994)], and computational modeling [L. Benuskova, M. E. Diamond, F. F. Ebner, *Proc. Natl. Acad. Sci. U.S.A.* **91**, 4791 (1994)].
19. M. Armstrong-James, C. A. Callahan, M. A. Friedman, *J. Comp. Neurol.* **303**, 193 (1991).
20. S.-M. Lu and C.-S. Lin, *Somatosens. Mot. Res.* **10**, 1 (1993).
21. M. E. Diamond, M. Armstrong-James, M. J. Budway, F. F. Ebner, *J. Comp. Neurol.* **319**, 66 (1992).
22. K. A. Hutson and R. B. Masterton, *J. Neurophysiol.* **56**, 1196 (1986).
23. M. H. Friedberg, thesis, Brown University (1991).
24. We thank D. Brown for assisting with histological processing and C. Porro for providing comments on the first draft of the manuscript. Supported by Whitehall Foundation award M93-12, National Institutes of Health award NS-25907, and the John F. Kennedy Center for Research on Education and Human Development.

31 March 1994; accepted 2 August 1994

Long-Term Potentiation: Evidence Against an Increase in Transmitter Release Probability in the CA1 Region of the Hippocampus

Toshiya Manabe* and Roger A. Nicoll†

It is widely accepted that *N*-methyl-D-aspartate (NMDA)–receptor–dependent long-term potentiation (LTP) in the CA1 region of the hippocampus is triggered postsynaptically, but there is considerable debate as to the site at which the increase in synaptic strength is expressed. The irreversible open-channel blocking action of the NMDA receptor antagonist MK-801 has been used to test whether the probability of transmitter release (P_r) is increased during LTP. Although the rate of decline of the amplitude of the NMDA receptor–mediated excitatory postsynaptic current (EPSC) in the presence of MK-801 strongly depends on P_r, the rate of decline of the EPSC evoked at synapses expressing LTP is identical to that observed at synapses not expressing LTP. These findings are difficult to reconcile with models in which the expression of LTP is due to an increase in P_r.

High-frequency activation of excitatory synapses in the CA1 region of the hippocampus results in an NMDA glutamate receptor–dependent, long-lasting increase in synaptic strength referred to as LTP (*1*, *2*). A variety of approaches have been used to determine whether the expression of LTP is pre- or postsynaptic, but the interpretation of the results has not been universally agreed upon (*2*). One approach has been to examine the interaction of LTP with paired-pulse facilitation (PPF), a phenomenon in which activation of a synapse at short intervals results in a presynaptic facilitation of transmitter release in response to the second stimulus (*3*). Although PPF is altered by a wide range of manipulations that increase P_r, there is no interaction between PPF and LTP (*4*, *5*). This finding has been used to argue for a postsynaptic site for LTP expression. However, if P_r increases with LTP, it is possible that the mechanism differs from that of other manipulations used to increase P_r and that this accounts for the lack of interaction between LTP and PPF.

To circumvent this problem, a direct method is needed to monitor changes in P_r that is entirely independent of the mechanism responsible for causing the change in P_r. Recently, two reports have described just such a method (*6*, *7*), which relies on the open-channel blocking action of the NMDA receptor antagonist MK-801 (*8*). Repeated activation of synapses in the presence of MK-801 results in a progressive decline in the amplitude of the NMDA receptor–mediated synaptic current. The rate of decay depends on P_r. When P_r is high, the decline is relatively rapid, because a large fraction of the synapses on a given stimulus release glutamate, which opens NMDA channels. These channels are then irreversibly blocked by the MK-801 and are unable to contribute to subsequent responses. We have used this approach to determine whether LTP has any effect on the rate of decay of the NMDA receptor–medi-

Departments of Pharmacology and Physiology, University of California, San Francisco, CA 94143, USA.

*Permanent address: Department of Neurophysiology, Institute for Brain Research, Faculty of Medicine, University of Tokyo, Tokyo, 113, Japan.
†To whom correspondence should be addressed.

ated component of the synaptic response in the presence of MK-801.

Whole-cell patch-clamp recording techniques were used in the in vitro hippocampal slice preparation (9). We first examined the effect of changing P_r on the decay of the NMDA excitatory postsynaptic current (EPSC) in the presence of MK-801 (Fig. 1). We recorded NMDA EPSCs in the presence of 6-cyano-7-nitroquinoxaline-2,3-dione (CNQX) and at a membrane potential of +50 mV, to remove the voltage-dependent block by Mg^{2+} (10). After establishing a stable base line at a stimulation of 0.1 Hz, the stimulator was turned off and MK-801 (40 μM) was applied. Stimulation was resumed 10 min later, and the NMDA EPSC was recorded in the continuous presence of MK-801. The size of EPSCs progressively diminished with a half decay time of 1.5 min, corresponding to nine stimuli (Fig. 1A). Sample records of the EPSCs (Fig. 1B) demonstrate that the time course of the EPSC speeds up in the presence of MK-801 (11) (see scaled trace with broken line in Fig. 1B). The time course of the EPSC is the same whether evoked early or late in the presence of MK-801, and thus the decline in the size of the EPSC cannot be due to an increase in the effective concentration of MK-801 during the observation period. When we decreased P_r by lowering extracellular Ca^{2+}, the decline in the EPSC in the presence of MK-801 was considerably slowed (Fig. 1C). The half decay time for the 2.5 mM Ca^{2+} experiments was 2.0 ± 0.2 min (n = 16), whereas for the 1.0 mM Ca^{2+} experiments it was 6.3 ± 0.9 min (n = 11) ($P < 0.00002$) (Fig. 1D). These findings confirm recent results both in hippocampal cultured neurons (6) and in slices (7).

How sensitive is this technique for detecting changes in transmitter release? A serious problem encountered in this study is that the decay varied substantially between slices even under the same conditions. Thus, in our standard 2.5 mM Ca^{2+} solution, the half decay time ranged from 0.9 to 3.4 min. This variation might be due to small differences in the physiological state of the slices, for example, varying concentrations of extracellular adenosine, which acts on presynaptic receptors, and differences in the effective concentration of MK-801 within the slice. The drug MK-801 is lipophilic, and therefore its concentration is unlikely to be uniform throughout the slice. Because the depth at which cells were recorded varied, it is likely that the effective concentration also varied.

We therefore sought a method that would permit the comparison of results from two pathways obtained from the same cell. First, we made sequential observations on separate pathways in the presence of MK-801, in which one pathway was analyzed as shown in Fig. 1, and then approximately 40 min later we analyzed a previously unstimulated input. However, this procedure failed because over this extended period the effective concentration of MK-801 increased, as witnessed by a faster decay time constant of the EPSC recorded later in the experiment (30.3 ± 2.2 ms for the first run versus 20.7 ± 2.0 ms for the second run, n = 3) and by the faster MK-801 block (half decay time of 2.5 ± 0.4 min for the first run versus 1.5 ± 0.4 min for the second run).

We next compared simultaneously two separate inputs onto the same cell. In this case, exactly the same decays were recorded for both pathways (Fig. 2A). Although this approach eliminated the interslice variability, a method had to be devised in which P_r could be varied selectively in one of the pathways so that the sensitivity of the approach could be ascertained. We accomplished this selectivity by applying paired-pulse stimulation to one of the pathways (Fig. 2B, inset). This treatment results in enhanced P_r from this pathway, and, as expected, the half decay time was clearly shorter (Fig. 2B). The half decay time for the control pathway (open triangles) was 2.3 ± 0.2 min and for the paired-pulse pathway (filled triangles) was 1.6 ± 0.2 min ($P < 0.0003$, n = 11).

The plot in Fig. 2B, which averages results across a number of slices, still suffers from the interslice variability. To overcome this problem, we compared the two pathways within a slice (Fig. 2C), and in each case the pathway with the paired-pulse stimulation decayed much faster than the control pathway. Thus, the points in Fig. 2C (triangles) clearly fall well below the diagonal line. On the other hand, when two pathways were stimulated alternately at the same frequency, synapses on the same cell showed very similar decay rates despite the substantial variability across slices; thus, the points (circles) fall close to the diagonal dotted line (Fig. 2C).

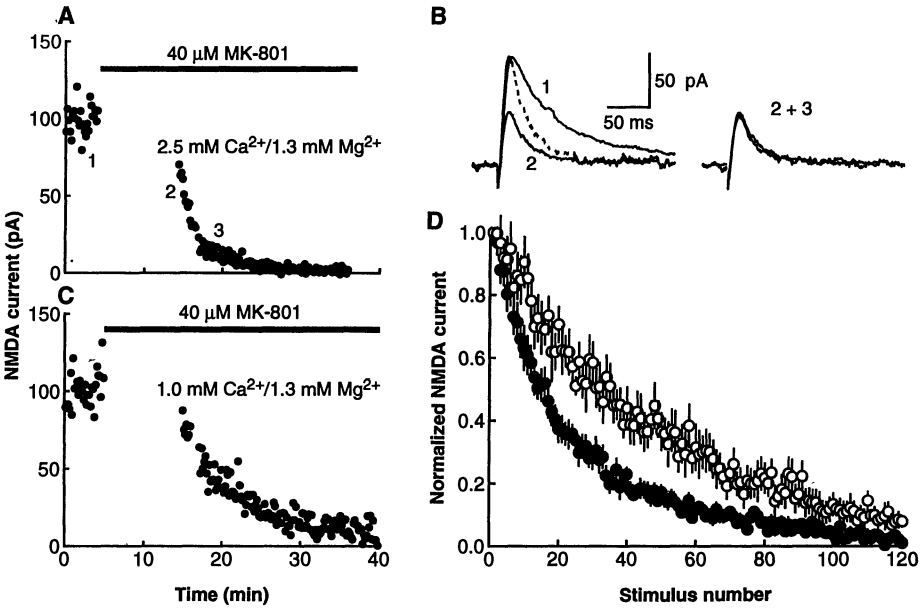

Fig. 1. The effect of the Ca^{2+}/Mg^{2+} ratio in the external solution on the decay time course of NMDA receptor–mediated EPSC amplitudes in the presence of MK-801 (9). Schaffer collateral-commissural afferent fibers were stimulated at 0.1 Hz in the presence of MK-801. (**A**) An example of blockade of NMDA receptor–mediated EPSCs by MK-801 in a solution containing a normal Ca^{2+}/Mg^{2+} ratio. Typically the response to the first stimulus in the presence of MK-801 was approximately 15% smaller than control values. Because of the slow rise time of the NMDA EPSC, it is possible that some channels could open and be blocked by MK-801 before the peak of the EPSC. (**B**) Sample traces of NMDA receptor–mediated EPSCs recorded from the cell illustrated in (A). Each trace is an average of six consecutive EPSCs recorded at the times indicated in (A). Trace 2 is the average of the first six EPSCs evoked in MK-801. The decay kinetics of NMDA receptor–mediated currents were much faster in the presence of MK-801 (trace 2) than before MK-801 application (trace 1). This difference is clearly shown when trace 2 is scaled to the peak of trace 1 (see trace with broken line), indicating that MK-801 was blocking open channels in a use-dependent manner. The trace recorded at time 3 is scaled to the trace at time 2 to compare the time course of the NMDA receptor–mediated currents. (**C**) An example of blockade of NMDA receptor–mediated EPSCs in a solution containing a low Ca^{2+}/Mg^{2+} ratio in a different cell. The decay time course was slower than under normal conditions, suggesting that a change in P_r could be detected by measuring parameters in the decay of NMDA receptor–mediated EPSC amplitude in the presence of MK-801. (**D**) Summary graph of this series of experiments. All the values are normalized in each experiment by the amplitude of the first EPSC evoked in the presence of MK-801 and averaged for each condition (filled circles: 2.5 mM $Ca^{2+}/1.3$ mM Mg^{2+}, n = 16; open circles: 1.0 mM $Ca^{2+}/1.3$ mM Mg^{2+}, n = 11).

In the two previous studies examining the use-dependent block of MK-801 on EPSCs (6, 7), it was proposed that P_r varies over a wide range among the population of synapses and, therefore, that synapses with a high P_r are the first synapses to be blocked by the MK-801. If this is the case, the recorded PPF should increase gradually as the high-P_r synapses are eliminated, leaving the low-P_r synapses with larger PPF. This is indeed the case, strongly supporting the heterogeneity in P_r among synapses and indicating that PPF enhances release to a greater extent on low-P_r synapses than on high-P_r synapses (Fig. 2D). An equivalent blockade of NMDA receptors by the competitive NMDA receptor antagonist APV (D,L-2-amino-5-phosphonovaleric acid) caused no change in PPF ($n = 4$).

We next addressed the issue of whether LTP is associated with an increase in P_r (Fig. 3). Two independent pathways converging onto the same postsynaptic cell were stimulated. The cell was held at −80 mV and the AMPA (α-amino-3-hydroxy-5-methyl-4-isoxazolepropionic acid) receptor–mediated EPSC was recorded. After establishing a base line for the two pathways, we induced LTP in one of the pathways by pairing synaptic stimulation with depolarization (Fig. 3, A and B). We then followed LTP for at least 60 min to determine that it was stable.

In addition, during this period of whole-cell recording the ability to induce LTP in the other pathway was washed out, while LTP, once induced, was unaffected (*12*). We confirmed this result by pairing the other pathway. This pairing ensured that, when we compared the two pathways in the presence of MK-801, one pathway would be expressing stable LTP while the other would be locked into a nonplastic state, although NMDA receptors were functional. To block the AMPA receptor response, CNQX was then applied, and the holding potential was shifted to a positive potential to record the NMDA synaptic response. After a stable base line was obtained, stimulation was stopped and MK-801 was applied. Synaptic stimulation was resumed after a 10-min period, and the responses to stimulation of the two pathways were compared (Fig. 3, C and D). In none of the six experiments was a clear difference in the decay of the NMDA EPSC seen between the two pathways. On average, the half decay time for the control pathway was 1.8 ± 0.1 min and 1.8 ± 0.1 min for the LTP pathway ($n = 6$) ($P > 0.9$).

To obtain a more precise comparison, uncontaminated by interslice variability, we compared the ratio of the half decay time of the control and LTP pathways against the magnitude of potentiation in each experiment. These points cluster around a half decay time ratio of 1 (filled circles in Fig. 4A). We compared these results with those obtained when we applied paired-pulse stimulation to one pathway and found that the half decay time ratios are well above 1 (open circles). The mean potentiation for the LTP experiments was 58 ± 9% and for the PPF experiments was 39 ± 6% (Fig. 4); the ratio of half decay times was 1.00 ± 0.05 for the LTP experiments and 1.49 ± 0.05 for the PPF experiments ($P < 0.00002$). This comparison indicates that, if P_r had changed with LTP, the technique was clearly sensitive enough to detect the change.

Although it is well established that paired pulses primarily facilitate release at synapses with low P_r, it is conceivable that LTP might increase P_r in an even smaller subset of synapses than occurs with PPF, in which case changes in the shape of the decay curve might be more prominent than differences in the half decay time ratios. A more accurate method for detecting small differences in the decay of two curves is to plot the size of responses of potentiated synapses as a function of the corresponding size of responses of the control synapses for each time point. If there is no difference in the two curves, the line described by these points ($y = a + bx + cx^2$) should be straight. For the PPF experiments (Fig. 4B), the deviation from linearity was striking ($c = -0.28 \pm 0.7$; $P < 0.004$). On the other hand, for the LTP experiments a straight line best describes the points ($c = 0.08 \pm 0.09$; $P > 0.4$, $n = 6$) (Fig. 4C). The values for c for the PPF and LTP experiments are significantly different ($P < 0.01$).

Another issue to keep in mind is that our method of analysis used the NMDA receptor component of the EPSC, although LTP is typically monitored on the AMPA receptor component. One possible scenario is that the ratio of NMDA to AMPA receptors varies greatly across synapses and that synapses with high ratios are already potentiated in control conditions, so that only

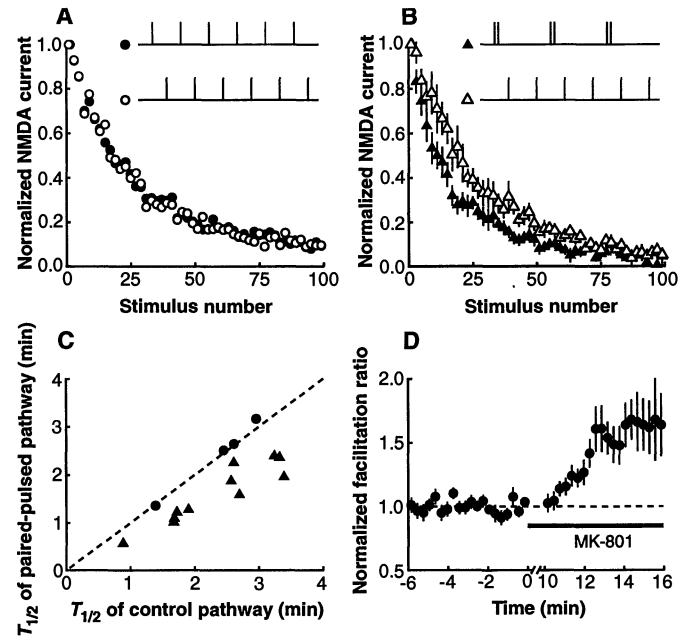

Fig. 2. Paired-pulse facilitation (PPF), a presynaptic phenomenon, accelerates the decay time course of NMDA-mediated EPSC amplitudes. We activated independent pathways by inserting two stimulating electrodes into stratum radiatum approximately 500 μm on either side of the recorded cell. (**A**) When two independent pathways (filled and open circles) were stimulated alternately at the same frequency (0.1 Hz) (see inset), EPSC amplitudes of the two pathways decayed with the same time course in the presence of MK-801. The result from one representative experiment is shown in this figure. (**B**) When one pathway (open triangles) was stimulated regularly at 0.1 Hz and another pathway (filled triangles) was given paired stimulation (inter-stimulus interval of 50 ms) at 0.05 Hz (see inset), which would selectively increase the P_r of the synapses in the latter pathway, the EPSCs evoked by the stimulation of the latter pathway decayed significantly faster than those of the former. Each pathway was given the same number of stimuli during the course of experiments. MK-801 (40 μM) had been applied for 10 min before the start of stimulation. Normalized EPSC amplitudes evoked by the first stimulus of the pair are plotted for the paired-pulsed pathway. For the control pathway the amplitude of the EPSC evoked by every other stimulus is plotted ($n = 11$). (**C**) Summary graph of this series of experiments. Triangles show the result of each of the individual experiments that form the summary graph in (B), in which paired stimulation was used. Half decay times ($T_{1/2}$) of NMDA receptor–mediated EPSC amplitudes of the control and paired-pulsed pathways were measured for each experiment. The half decay time of the paired-pulsed pathway was significantly shorter ($P < 0.00003$) than that of the control. Circles show the result of each of the individual control experiments, one of which is shown in (A), where both pathways received exactly the same stimulation. There was no significant difference ($P > 0.25$) in half decay times between the two pathways ($n = 4$). (**D**) Effect of MK-801 on PPF. PPF recorded in the experiments shown in (B) was normalized over the 6-min control period. After 10 min, MK-801 (40 μM) was applied for 10 min and stimulation was then resumed. In the presence of MK-801, PPF gradually increased with the stimulus number, suggesting that synapses with low P_r were on average being preferentially spared, which supports the idea that subpopulations of synapses with different P_r values exist.

synapses with low ratios can express LTP. If this were to occur, possible effects of LTP on the decay of the NMDA component might be more difficult to observe.

The present results put severe constraints on possible mechanisms responsible for the expression of LTP in the CA1 region of the hippocampus. They appear to make a change in P_r unlikely to contribute importantly to the increase in synaptic strength. An increase in the number of release sites is theoretically possible but would require that these new release sites be on synapses that before LTP were entirely silent; otherwise a recruitment of additional release sites would, on average, increase the overall probability of release at that synapse, which would be detected by the MK-801. Thus, the present results favor a postsynaptic mechanism of expression.

How can the present results be reconciled with studies using quantal analysis (*12*, *13*)? A number of studies have reported a decrease in the incidence of failures of transmission after LTP, although the failure rate has not been examined in detail at time periods equivalent to those used in the present study. The decrease in failures is usually interpreted as an increase in P_r. Alternatively, the decrease in failures could reflect the appearance of patches of functional AMPA receptors on the postsynaptic cell.

In summary, although our use of the irreversible open-channel blocking action of MK-801 provided a sensitive assay for changes in P_r, we were unable to detect any effect of LTP on P_r. This result favors an LTP expression mechanism involving an increase in postsynaptic sensitivity to glutamate.

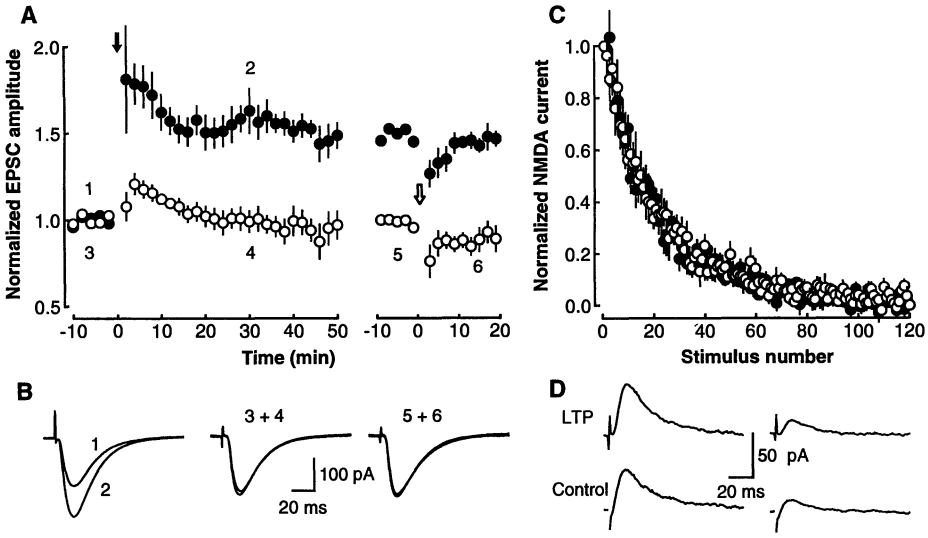

Fig. 3. The effect of LTP on the decay time course of NMDA receptor–mediated EPSC amplitudes in the presence of MK-801. (**A**) Summary graph of six experiments. The first pairing (filled arrow) caused a stable LTP in one pathway (filled circles), whereas the second pairing (open arrow) in the other pathway (open circles) failed to induce any potentiation, presumably the result of washout of the LTP-inducing mechanism. In all six cells we applied CNQX after confirming that the second pathway had lost the ability to show LTP. (**B**) Sample traces of AMPA receptor–mediated EPSCs (average of 10 traces) recorded from one of the cells shown above. We induced LTP in one pathway by pairing depolarization to 0 mV with electrical stimulation of afferent fibers at 2 Hz for 20 s. In the other pathway the same pairing was given at least 60 min after the whole-cell recording was obtained. (**C**) The decay of NMDA receptor–mediated EPSC amplitudes in the LTP pathway (filled circles) in the presence of MK-801 was superimposable on that in the control pathway (open circles). Half decay times of the LTP pathway were not statistically different from those of the control pathway ($P > 0.9$). (**D**) Sample records of NMDA receptor–mediated EPSCs (average of six traces) from one cell are shown. We recorded the left traces just after starting stimulation in the presence of MK-801 and the right traces around the 25th stimulation.

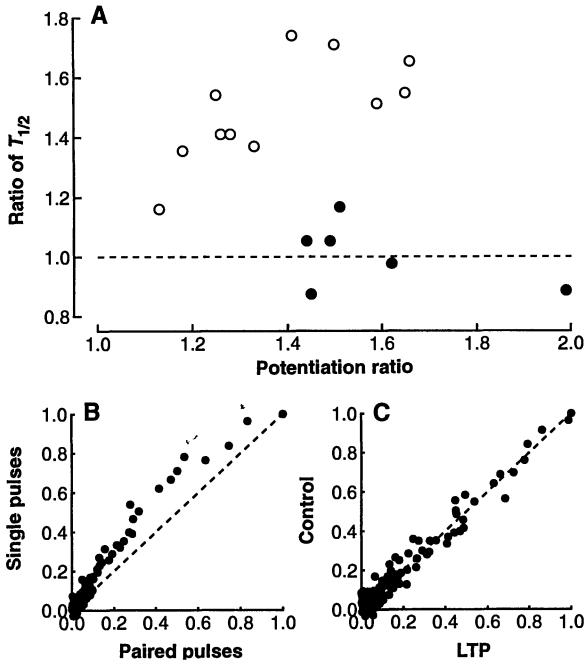

Fig. 4. Summary graphs comparing the effects of LTP and PPF. (**A**) The ratio of the half decay time ($T_{1/2}$) of the control pathway to that of the potentiated pathway plotted as a function of the potentiation ratio. Although PPF showed a clear increase in the ratio of the half decay time (open circles), LTP failed to show any change (filled circles). The potentiation ratio in PPF experiments was expressed as half of the recorded PPF in control conditions because the first of the responses induced by paired stimulation should be unaffected by this manipulation. The potentiation ratios were obtained before the addition of MK-801. (**B**) Plot of the size of the normalized response in the control pathway as a function of the size of the normalized response in the pathway receiving paired pulse stimulation for each time point. The initial responses in the presence of MK-801 are displayed at the upper right corner of the graph, and the final points are near the origin. (**C**) The size of the normalized response in the control pathway plotted against the size of the normalized response in the pathway expressing LTP.

REFERENCES AND NOTES

1. T. V. P. Bliss and G. L. Collingridge, *Nature* **361**, 31 (1993); D. V. Madison, R. C. Malenka, R. A. Nicoll, *Annu. Rev. Neurosci.* **14**, 379 (1991).
2. R. A. Nicoll, D. J. A. Wyllie, T. Manabe, D. J. Perkel, in *Cellular and Molecular Mechanisms Underlying Higher Neural Functions*, P. Ascher and A. I. Selverston, Eds. (Wiley, Chichester, England, 1994), pp. 189–202; M. Baudry and J. L. Davis, Eds., *Long-Term Potentiation: A Debate of Current Issues* (MIT Press, Cambridge, MA, 1991).
3. A. Mallart and A. R. Martin, *J. Physiol.* **196**, 593 (1968); R. Creager, T. Dunwiddie, G. Lynch, *ibid.* **299**, 409 (1980); R. S. Zucker, *Annu. Rev. Neurosci.* **12**, 13 (1989).
4. B. L. McNaughton, *J. Physiol.* **324**, 249 (1982); B. Gustafsson, Y.-Y. Huang, H. Wigström, *Neurosci. Lett.* **85**, 77 (1988); D. Muller and G. Lynch, *Brain Res.* **479**, 290 (1989); R. A. Zalutsky and R. A. Nicoll, *Science* **248**, 1619 (1990) [but see L. L. Voronin and U. Kuhnt, *Neurosci. Res. Commun.* **6**, 149 (1990)].
5. T. Manabe, D. J. A. Wyllie, D. J. Perkel, R. A. Nicoll, *J. Neurophysiol.* **70**, 1451 (1993).
6. C. Rosenmund, J. D. Clements, G. L. Westbrook, *Science* **262**, 754 (1993).
7. N. A. Hessler, A. M. Shirke, R. Malinow, *Nature* **366**, 569 (1993).
8. J. E. Huettner and B. P. Bean, *Proc. Natl. Acad. Sci. U.S.A.* **85**, 1307 (1988).
9. Male Hartley guinea pigs 3 to 5 weeks old were decapitated under halothane anesthesia, and hippocampi were quickly removed. Standard procedures and solutions were used to prepare the slices and whole-cell pipettes (*5*). When NMDA receptor–mediated EPSCs were recorded, CNQX (10 μM) was present throughout the experiment to block AMPA receptor–mediated EPSCs. MK-801 (40 μM) (Research Biochemicals, Natick, MA) was applied to the perfusing solution. The values of membrane potential have not been corrected for the liquid-junction potential at the electrode tip. Series and input resistances were monitored throughout the experiment. To evoke synaptic currents, we delivered stimuli through fine bi-

polar stainless steel electrodes placed in the stratum radiatum. Stimuli were delivered at 0.1 Hz unless otherwise stated, and stimulus strength remained constant throughout the experiment. We measured EPSC amplitudes by averaging a 10-ms window around the peak and subtracting the average value obtained during a 10-ms window immediately before the stimulus. We measured the amplitudes of the second EPSCs evoked by paired stimulation in the same way after subtracting an averaged scaled trace, obtained from the pathway that was given single stimuli, from the trace obtained with paired stimulation. The data are expressed as means ± standard errors of the mean. Student's t test was used to determine whether there was a significant difference in the mean between two sets of data.

10. Although the dissociation of MK-801 from the channel is facilitated at positive membrane potentials (*8*), unblocking was minimal in our experiments because little recovery of the blocked NMDA EPSC occurs during a 40-min period after washout of MK-801 (n = 3).
11. S. Hestrin, P. Sah, R. A. Nicoll, *Neuron* **5**, 247 (1990).
12. R. Malinow and R. W. Tsien, *Nature* **346**, 177 (1990).
13. J. M. Bekkers and C. F. Stevens, *ibid.*, p. 724; R. Malinow, *Science* **252**, 722 (1991); T. C. Foster and B. L. McNaughton, *Hippocampus* **1**, 79 (1991); D. M. Kullmann and R. A. Nicoll, *Nature* **357**, 240 (1992); D. Liao, A. Jones, R. Malinow, *Neuron* **9**, 1089 (1992); A. Larkman, T. Hannay, K. Stratford, J. Jack, *Nature* **360**, 70 (1992).

14. We thank Z. Hall, S. Hestrin, D. Perkel, M. Stryker, and D. Wyllie for comments on the manuscript. This work was supported by grants from the National Institute of Mental Health. R.A.N. is a member of the Keck Center for Integrative Neuroscience and the Silvio Conte Center for Neuroscience Research.

4 May 1994; accepted 2 August 1994

TECHNICAL COMMENTS

Retention of Helium in Subducted Interplanetary Dust Particles

I welcome the report by H. Hiyagon (*1*) of diffusive loss of He and Ne from interplanetary dust particles (IDPs) as a significant contribution to the evaluation of Anderson's hypothesis (*2*) that the high $^3He/^4He$ ratios in ocean island basalt (OIB) hotspots reflect He introduced into the mantle by subduction of IDP-containing sediments. Hiyagon's measurements of the high diffusivities of He and Ne in IDPs at the temperatures of subducting slabs should lay this proposal (*2*) to rest.

Here I wish to comment on the results of the diffusion experiments with particular reference to the deviations of the measured diffusivities from a linear Arrhenius plot at the low-temperature end of the data (500 and 600°C). The samples used in these experiments were magnetite separates from Pacific Ocean sediments. Hiyagon's measurements show that the diffusivities of both He and Ne are significantly greater at 500 and 600°C than are the values predicted by the close fit to a linear Arrhenius plot of data measured at higher temperatures. I believe this is a result of conversion of some of the magnetite to metallic α-iron at the lower temperatures. In the high-temperature experiments magnetite would be converted by deoxidation to wüstite ($FeO_{.95}$) and magnetite, which should have only a minor effect on diffusive loss of gases.

Figure 1 shows the Fe-O phase diagram (*3*) at the temperatures of interest, 400 to 1200°C, the highest temperature at which diffusive loss was measured. At $T < 560$°C, pure magnetite lies on the boundary between the two-phase regions (magnetite + hematite) and (magnetite + α-iron). At ~500°C, pure magnetite is stable over the range of equilibrium gas compositions given by $p(O_2) = 10^{-18}$ to 10^{-29} bars, $p(H_2)/p(H_2O) = 10^{-5}$ to 3.2, and $p(CO)/(CO_2) = 2 \times 10^{-6}$ to 1, these being the limiting values between the two-phase stability fields (magnetite + hematite) and (magnetite + α-iron), respectively (*4*). Thus, under the high-vacuum conditions of the experiments (*1*), low O_2 fugacities and high CO/CO_2 and H_2/H_2 ratios will shift pure magnetite into the stability field of magnetite + α-iron. The relevant equilibria are:

$$Fe_3O_4 = 3Fe(\alpha) + 2O_2$$

$$Fe_3O_4 + 4CO = 3Fe(\alpha) + 4CO_2$$

The effect of these reactions on diffusive gas loss is due to the large density change in the conversion of magnetite (ρ = 5.2) to metallic Fe (ρ = 7.9), resulting in a large volume decrease that strongly enhances diffusive loss of gases. Observations (*5*) show that in the conversion of magnetite to metallic iron the magnetite grains become deeply fissured with a large increase of surface area per unit volume, which significantly increases the rate of diffusive gas loss. In the experiments above 600°C, however, the stable phases on deoxidation become magnetite and wüstite (ρ = 5.75), and conversion to wüstite is accompanied by a negligible volume change with no fissuring (*5*), and thus no enhanced diffusive loss of gases.

In sediments undergoing subduction the environment is highly anoxic and magnetite will undergo at least partial direct reduction to Fe at lower temperatures, followed at higher temperatures by a two-stage reduction to wüstite and then to metallic Fe (Fig. 1). The mechanisms involved have been described in detail (*5*) and show that diffusive loss will also be enhanced by fissuring at the higher temperatures when deoxidation reaches the stage of conversion of wüstite to metallic iron. Therefore the measured diffusive losses (*1*), under conditions probably not reached in the higher-temperature experiments but certainly achieved in subducted sediments, should be regarded as *lower limits* for the actual diffusive loss rates in subducted IDPs. A final, and ultimately conclusive experiment on diffusion losses could be carried out by mixing an IDP concentrate back into a small volume of the original sediment (reduced to fit the experimental apparatus) and measuring diffusive losses and temperature directly, and in a sealed container in which CO, CO_2, and O_2 fugacities are controlled within limits appropriate to sediments in subducting slabs. Examination of the magnetite residues from the various heating cycles would document the phase changes resulting from deoxidation with the diffusion losses of He and Ne in each experiment.

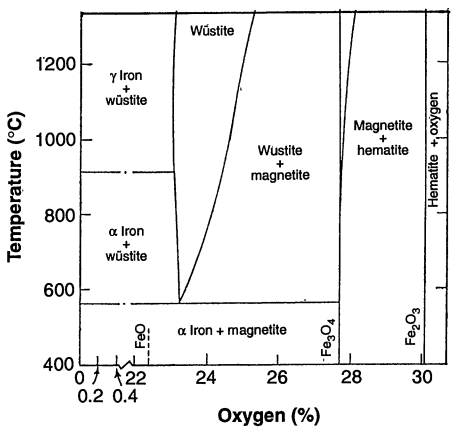

Fig. 1. Fe-O phase diagram at 400 to 1200°C (*3*). Oxygen values are in weight percent.

Nevertheless, it appears certain from the present experimental results (*1*) that He and Ne in IDPs cannot survive the subduction process to become significant components in the upper mantle. Observations on mantle-derived basalts in subduction arc regimes reinforce this conclusion: the $^3He/^4He$ ratios observed in all the major circum-Pacific arc volcanic gases and basalts (*6*) are always at least equal to, and generally lower than, the ratios in the worldwide reservoir tapped by mid-ocean ridge basalt (MORB) lavas. In some arcs, such as Indonesia, the ratios are much lower, indicating the incorporation of radiogenic helium from continental sources (*7*). If He with the high $^3He/^4He$ ratios characteristic of IDPs were to survive the subduction process, one would expect to observe ratios greater than those of MORBs, if anywhere, in the lavas and volcanic gases derived from the mantle wedge above the subducting slabs, where He accumulates by volatile transport from the downgoing slab. However, $^3He/^4He$ ra-